Digital Object Identifier: 10.1109/ULTSYM.2008.0239

Spectral and temporal signal modifications occuring between stable and transient inertial cavitation

Mathieu Santin, S. Lori Bridal
Laboratoire d'Imagerie Paramétrique
Université Pierre et Marie Curie, CNRS UMR 7623
15 rue de l'Ecole de Médecine, 75006 Paris, France
santin@lip.bhdc.jussieu.fr

Alexander Haak, W. D. O'Brien Jr.
Bioacoustics Research Laboratory
Department of Electrical Engineering
University of Illinois, 405 North Mathews
Urbana, IL 61801, USA

Abstract— **The goal of this work is to investigate temporal and spectral modifications in passive cavitation detection (PCD) measurements from ultrasound contrast microbubbles (MBs) related to MB rupture. Contrast MB pressure-time responses are modelled with the Marmottant model. Results demonstrate that post-excitation signals occur on simulated pressure-time traces for MBs only when radial oscillations exceed the modelled break-up radius within a range of sizes near the resonant size. PCD signals are acquired from MBs of Optison, Definity and Sonovue (acoustic excitation at 2.8-MHz, 5-cycle transmit; confocal 13-MHz receiver). Although data are acquired at relatively high incident acoustic pressures (peak rarefactional pressure of 1.6, 2.0 and 2.4 ± 0.2 MPa), subsets of data with and without post-excitation signals are identified for each MB type and pressure range. Post-excitation signals are used to identify which PCD signals indicate MB break-up [1] then average values of peak-to-peak voltage, 2nd harmonic, 3rd and 4th harmonic and broadband noise are calculated for responses from groups of ruptured and nonruptured MBs for each pressure range and MB type. The signal to noise ratio (SNR) is high (10 to 49 dB) both for ruptured (with post-excitation signals) and nonruptured (no post-excitation signals) MBs for all pressures and MBs. The average parameter values from ruptured MBs are approximately 3 to 8 dB higher than for nonruptured MBs although differences vary with the type of MB. Results contribute to better understand the link between PCD spectral and temporal modifications and MB break-up.**

Microbubble, Rupture, Inertial Cavitation, Marmottant

I. INTRODUCTION

PCD is widely applied in research to detect inertial cavitation (IC). Detection is sometimes based on features of the voltage-time signal such as increases in the rms or peak voltages [2]. Many other PCD-based studies have applied criteria based on increased voltage levels or broadband power to characterize IC thresholds [3-5]. Although, the specific harmonic content of PCD received signals and their modification when IC occurs has remained largely unexplored, it has been demonstrated that subharmonic, second and third harmonic peaks may also be modified near IC thresholds [6,7].

Thus, a large variety of temporal and spectral criteria have been utilized to assess IC activity. Because of the myriad approaches and because increased PCD voltage and spectral power levels may result from IC with or without microbubble (MB) rupture, ambiguity persists concerning the precise nature of the MB response at the IC thresholds reported in the literature. Better understanding of spectral or temporal modifications linked to IC and specifically linked to MB break-up could help link this break-up to bioeffects observed in vivo, and ultimately, could be used to better gage and control therapy.

In previous work, we utilized PCD to evaluate isolated Optison MBs. Post-excitation signals in the voltage-time signal were linked to shell rupture [1] (transient IC associated with MB break-up). Spectral content and the presence of broadband emissions were not systematically studied in the previous work.

The goal of the current work is to provide an original look at the changes in the temporal and spectral response for ruptured versus nonruptured MBs. Theoretically modeled [8] pressure-time and spectral responses were examined to investigate the relationship between bubble break-up, pressure-time response and MB size. PCD signals from dilute solutions of Optison, Definity and Sonovue MBs were acquired at strong incident pressures (1.6 to 2.4 MPa, peak rarefactional pressure) sufficient to promote MB IC response. These signals were analyzed to identify modifications of harmonic and broadband acoustic emissions as well as peak-to-peak voltages linked specifically to MB break-up.

II. MATERIALS AND METHODS

A. Microbubbles

Three contrast agent microbubbles were used: Optison (Amersham Health), Sonovue (Bracco Diagnostics, Inc.) and Definity (Bristol-Myers Squibb Medical Imaging Inc.). Both Optison and Definity have an octofluoropropane C_3F_8 gas core whereas Sonovue has a sulfurhexafluoride SF_6 core. Optison's shell is made of human serum albumin and N-acetyltryptophan caprylic acid. Sonovue and Definity have shells based on different phospholipids [9].

B. Theoretical modelling

To model MB response, we used the model proposed by Marmottant to describe behavior of lipid coated MBs, considering that the shell of the bubble buckles for bubble radii R below $R_{buckling}$ and breaks-up for R greater than $R_{break\text{-}up}$. This model leads to the dynamic equation:

$$\rho_l\left(R\ddot{R}+\frac{3}{2}\dot{R}^2\right)=\left[P_0+\frac{2\sigma(R_0)}{R_0}\right]\left(\frac{R}{R_0}\right)^{-3\kappa}\left(1-\frac{3\kappa}{c}\dot{R}\right) - \frac{2\sigma(R)}{R}-\frac{4\mu\dot{R}}{R}-\frac{4\kappa_S\dot{R}}{R^2}-\left(P_0+P_{ac}(t)\right) \quad (1)$$

with a surface tension $\sigma(R)$ defined as:

$$\sigma(R)=\begin{cases}0 & if\ R\le R_{buckling}\\ \chi\left(\frac{R^2}{R_{buckling}^2}-1\right) & if\ R_{buckling}\le R\le R_{break-up}\\ \sigma_{water}=0.073N/m & if\ broken\ and\ R\ge R_{ruptured}\end{cases} \quad (2)$$

Radiated pressure $P(t)$ of the MB was computed from radial displacement, velocity and acceleration as defined in [10] . Pressure-time signals were filtered by the impulse response of the receive transducer used in the PCD system for comparison with experimental results.

In the above equations, ρ_l is the density of the surrounding liquid, P_0 the ambient pressure, κ the polytropic gas exponent, c, the speed of sound in the liquid, μ the liquid viscosity, χ the shell elasticity, κ_s the shell viscosity and $P_{ac}(t)$ the acoustic pressure at time t measured with the hydrophone. It is possible with this model to adjust the break-up radius by varying the maximum surface tension limit. The model was first used to to simulate bubble expansion at low incident pressure to identify which size of MBs resonates at the insonification frequency used in our PCD measurements.

Pressure-time responses were then simulated at a driving peak rarefactional pressure of 2.0 MPa (2.8 MHz, 5-cycles) under the assumption that $R_{break\text{-}up}=2R_0$ for Definity and Sonovue. This break-up radius was chosen based on the radial expansion criterion defined for collapse threshold of gas bubbles by Flynn [11] and Church [12]. The break up threshold was lowered for Optison simulations ($R_{break\text{-}up}=1.5R_0$).

C. Passive Cavitation Detector

Dilute solutions of ultrasound contrast agents were studied using a PCD with a 2.8-MHz transmitter and 13-MHz receiver. Details describing this system have been provided previously [1]. Incident peak rarefactional pressure was characterized for each emitter setting in a separate experiment using a calibrated PVDF bilaminar shielded membrane hydrophone (0.5-mm diameter, 699/1/00001/100, GEC Marconi Ltd., Great Baddow UK) placed at the focal point. The dilution of the MBs was such that each signal received by the 13-MHz receiver should, on average, arise from a single MB within the confocal volume determined by the intersecting volume of the two -6dB beam volumes. MB responses (N ≥ 100) were acquired within each of three incident rarefactional pressure ranges (1.6 ± 0.2, 2.0 ± 0.2 and 2.4 ± 0.2 MPa). A 5-cycle transmit pulse was used throughout the study.

D. Data Analysis

Within each of the selected incident pressure ranges, the microbubble responses that presented a clear principle response with no post-excitation signal (oscillation during acoustic excitation only) were classified as nonruptured MB. Those that presented a clear principle response followed by a post-excitation emission after the principle response were classified as ruptured MB. The average spectral density and the average peak-to-peak voltage values were calculated for the group of N_t signals in a selected incident pressure range with post-excitation emissions (ruptured MB group). The same average parameters were calculated for the group of N signals with no evidence of post-excitation emission (nonruptured MB group). The group selection criteria and steps towards calculation of average parameters are illustrated schematically in Fig 1.

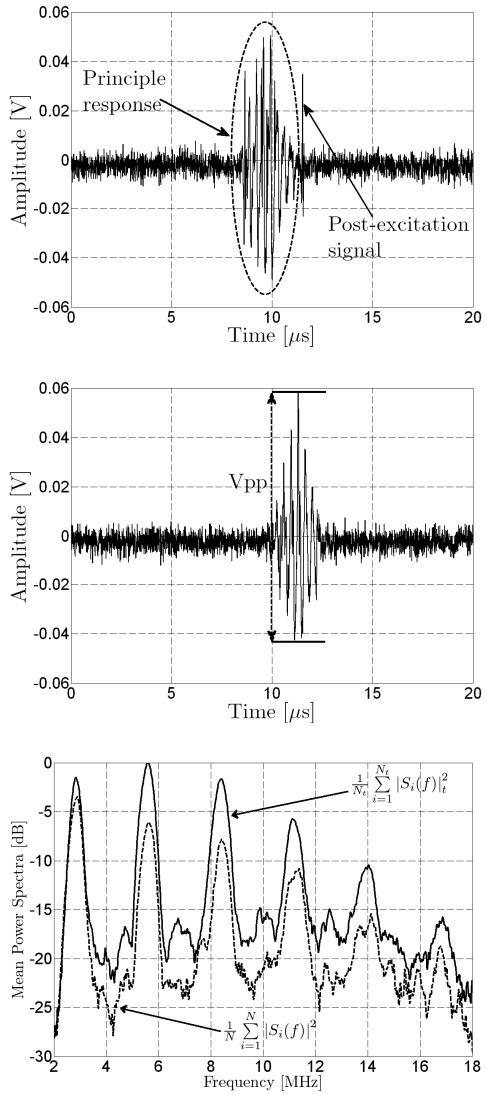

Figure 1. Illustration of group selection criteria and the steps for parameter computation. The signals shown were acquired with the PCD system from Definity insonified at an incident peak rarefactional pressure within the range of 2.0 ± 0.2 MPa (5 cycles, 2.8 MHz). Top: signal presenting a post-excitation signal after the principle response during acoustic excitation. This type of signal was classified in the group for ruptured MBs. The principle response and the post-excitation signal are indicated. Middle: example presenting no

post-excitation signal. This type of signal was classified in the group nonruptured MBs. The peak-to-peak voltage measurement is demonstrated graphically. Bottom: The average power spectral density for ruptured MBs (N_t=18) and the nonruptured MB groups (N=17).

For each incident pressure range, we compared discrimination between these two groups based on peak-to-peak voltage, broadband noise, power at the fundamental, 2nd, 3rd and 4th harmonic peaks. For spectral power comparisons, the average value of the power was measured in the following bandwidths: broadband noise, 12-17.6 MHz; fundamental, 2.6 to 3 MHz; 2nd harmonic, 5.3 to 5.9 MHz; 3rd harmonic, 8 to 8.8 MHz and 4th harmonic 10.7 to 11.7 MHz. These bandwidth limits are approximately –6 dB down from the peak values. Noise levels were estimated from the peak-to-peak voltage and power levels in the spectral density calculated for segments of signals acquired at the same insonification settings in the absence of contrast microbubbles (water only).

III. RESULTS

A. Modelling

Pressure-time responses simulated for three different initial radii (radius at resonance, far below resonance and far greater than resonance) for Definity and Sonovue. Results for Definity are presented in Fig. 2. The pressure-time response for the resonant radius satisfies the criterion fixed for rupture ($R_{max} > 2R_0$) in Eq. (2) while the pressure-time responses for the radii far from resonance do not. It can be seen in Fig. 2 that the pressure-time curve at resonance presents a post-excitation signal whereas the others do not. Same behaviour was found on Sonovue.

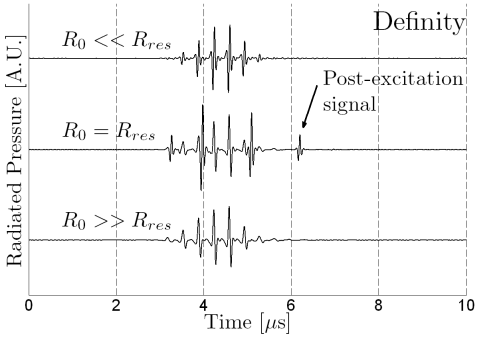

Figure 2. Simulated radiated pressure for a Definity microbubble at 3 different initial radii. Simulations were performed using Eq. 1 and the surface tension described in Eq. 2. From top to bottom the response is simulated for bubbles with radii R_0 = 0.82 ; 2.14; 6.00 µm. The break-up radius R_{break} = $2R_0$ is only exceeded for the bubble at resonance radius.

In spite of the fact that the break-up radius assigned for Optison ($R_{break\text{-}up}$=1.5R_0) was exceeded at resonance, application of Eqs. (1-2) did not yield pressure-time responses with post-excitation signals at resonance. Eqs. (1-2) are based on behavior of lipid-based shells and assumes that the shell parts remain and recombine across the MB surface during recompression after shell break-up.

When Optison's albumin shell breaks the remains are not likely to behave in the same manner as for a more flexible lipid-shelled agent [13] and fragments may not be able to recombine. Based on this, surface tension conditions described in Eq. (2) were modified so as to permanently fix $\sigma(R) = \sigma_{water}$ and thus to suppress the shell viscosity term once $R = R_{break\text{-}up}$ was reached for the first time, giving:

$$\sigma_{defbreak\text{-}up}(R) = \begin{cases} 0 & \text{if } R \le R_{buckling} \text{ and shell not broken} \\ \chi\left(\frac{R^2}{R_{buckling}^2} - 1\right) & \text{if } R_{buckling} \le R \le R_{break\text{-}up} \text{ and shell not broken} \\ \sigma_{water} = 0.073 N/m & \text{once broken} \end{cases} \quad (3)$$

Applying this modified equation to describe the surface tension, post-excitation signals were observed in simulated pressure-time responses for Optison MBs at resonance when $R_{max} \geq 1.5\ R_0$ but not for MBs far from resonance where more limited oscillations occurred (Fig. 3).

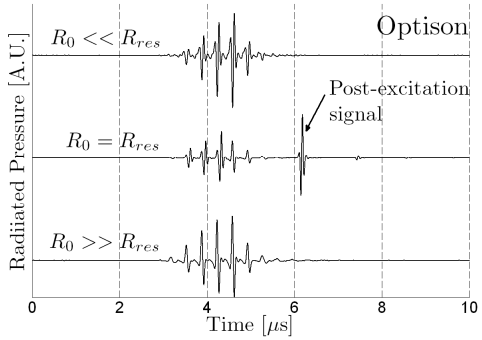

Figure 3. Simulated radiated pressure for an Optison microbubble at 3 different initial radii. Simulations were performed using Eq. 1 and the surface tension as described in Eq. 3. From top to bottom the response is simulated for bubbles with radii R_0 = 1.00 ; 2.6; 7.00 µm. The break-up radius R_{break} = $1.5R_0$ is only exceeded for the bubble at resonance radius.

B. PCD Measurements

For each MB, the average spectral and temporal parameter values are compared for ruptured and nonruptured groups as a function of incident pressure in Fig. 7. Spectral power values for the two groups tend to be separated by less than 4.0 dB at the fundamental frequency. Mean values of peak-to-peak voltage as well as 2^{nd}, 3^{rd}, 4^{th} harmonics and broadband noise are generally higher for the transient IC group than for the nonruptured bubble group. With increasing incident pressure, the SNR for each parameter tends to increase but the differences between values for ruptured and nonruptured MBs are approximately maintained.

For Optison, the greatest differences (average for three different incident pressure ranges) between ruptured and nonruptured MBs were obtained with peak-to-peak voltage (4.7 ± 1.8 dB) and broadband noise (5.6 ± 2.2 dB).

For Definity MBs, peak-to-peak voltage (5.3 ± 0.9 dB) and broadband noise (5.7 ± 1.4 dB). were also more elevated in the ruptured MB group than the nonruptured group. Furthermore, the 2^{nd} and 3^{rd} harmonics were higher (on the order of 6dB) in

the ruptured MB group with respect to the nonruptured MB group. For Sonovue, peak-to-peak voltage and broadband noise were 7.3 ± 2.3 dB and 5.4 ± 1.4 dB, respectively, higher for the ruptured MB group than for nonruptured MBs. The 2^{nd}, 3^{rd} and 4^{th} harmonics were more elevated in the ruptured Sonovue MB group, respectively, 8.3 ± 0.1, 7.9 ± 1.7 and 7.9 ± 3.0 dB.

IV. SUMMARY

The aim of this work is to investigate what temporal or spectral modifications in PCD measurements from ultrasound contrast microbubbles can be linked to MB rupture. Three contrast agent MBs were considered: Optison, Sonovue and Definity. Modelling of the pressure-time response using the model developed by Marmottant et al demonstrated that post-excitation signals occur for MBs at or near the resonant radius when radial oscillation exceeds the break-up threshold. Modelled responses for MBs with oscillations not exceeding the break-up threshold did not present post-excitation signals. Post-excitation signals in experimental PCD data were used to separate MB rupture and nonruptured microbubble oscillation events. Although all data were acquired at relatively high incident acoustic pressure (1.6 to 2.4 MPa) , it was possible to identify subsets of data with and without post-excitation signals for each studied agent and pressure range. The SNR ratio measured from PCD data was strong (9.9 to 49.1 dB) for all spectral and temporal parameters both for ruptured and nonruptured MBs. The response from ruptured MBs presented on the order of 3.2 to 8.3 dB additional power for most agents and parameters relative to the response from nonruptured MBs.

Pressure-time response calculated using the model developed by Marmottant et al provides a good description of experimentally observed post-excitation signals when the model parameters are fixed to allow rupture of a lipid-shelled agent. Post-excitation signals can also be obtained with this model for non-lipid shelled agents but only after modifying the shell parameters to eliminate shell viscosity and surface tension for all time after $R_{break\text{-}up}$ is initially reached.

REFERENCES

[1] A. Ammi, R.O. Cleveland, J. Mamou, G. Wang, S.L. Bridal, W. D. O'Brien Jr. "Ultrasonic contrast agent shell rupture detected by inertial cavitation and rebound signals", IEEE Trans Ultrason. Ferroelectr. Freq. Control **53**, 126 (2006).

[2] C. Rota, C.H. Raeman, S. Z. Child. D. Dalecki "Detection of acoustic cavitation in the heart with microbubble contrast agents in vivo: A mechanism for ultrasound-induced arrhythmias", J. Acoust. Soc. Am. **120**, 2958 (2006)..

[3] E. Sassaroli, K. Hynynen "Cavitation threshold of microbubbles in gel tubes by focused ultrasound", Ultrasound Med. Biol. **33**, 1651 (2007).

[4] C.-Y. Lai, C.-H. Wu, C.-C- Chen, P.-C. Li "Quantitative relations of acoustic inertial cavitation with sonoporation and cell viability", Ultrasound Med. Biol. **32**, 1931 (2006).

[5] J. Tu, J. H. Hwang, T. J. Matula, A. A. Brayman, L. A. Crum "Intravascular inertial cavitation activity detection and quantification in vivo with Optison", Ultrasound Med. Biol. **32**, 1601 (2006).

[6] N. McDannold, N. Vykhodtseva, K. Hynynen "Targeted disruption of the blood-brain barrier with focused ultrasound: association with cavitation activity", Phys. Med. Biol. **51**, 793 (2006).

[7] E. Biagi, L. Breschi, E. Vannacci, L. Masotti "Stable and transient subharmonic emissions from isolated contrast agent microbubbles", IEEE Trans Ultrason. Ferroelectr. Freq. Control **54**, 480 (2007).

[8] P. Marmottant, S. Van der Meer, M. Emmer, M. Versluis, N. de Jong, S. Hilgenfeldt, D. Lohse "A model for large amplitude of coated bubbles accounting for buckling and rupture", J. Acoust. Soc. Am. **118**, 3499 (2005).

[9] A. P. Miller, N. C. Nanda "Contrast echocardiography: new agents", Ultrasound Med. Biol. **30**, 425 (2004).

[10] T.G. Leighton "The Acoustic Bubble", Academic, London, 1994.

[11] H. G. Flynn "Cavitation Dynamics. II. Free pulsations and models for cavitation bubbles", J. Acoust. Soc. Am. **58**, 1160 (1975).

[12] H. G. Flynn, C. C. Church "Transient pulsations of small gas bubbles in water", J. Acoust. Soc. Am. **72**, 1926 (1988).

[13] J. E. Chomas, P. Dayton, K. Morgan, J. Allen, K. W. Ferrara "Mechanisms of contrast agent destruction", IEEE Trans Ultrason. Ferroelectr. Freq. Control **48**, 232 (2001).